

## Theory of light-induced drift of electrons in coupled quantum wells

Mark I. Stockman,\* Leonid S. Muratov,\* and Thomas F. George

*Department of Physics, Washington State University, Pullman, Washington 99164-2814  
and Department of Chemistry, Washington State University, Pullman, Washington 99164-4630*

(Received 23 April 1992)

A theory of the new effect of light-induced drift (LID) in coupled potential wells is developed on the basis of the density-matrix method. The effect appears when light excites intersubband electronic transitions. LID manifests itself as the photocurrent of the two-dimensional electron gas in the well plane, which depends on coherent electron tunneling between the coupled wells. The theory shows the effect to possess distinctive features such as a characteristic antisymmetric spectral contour consisting of four alternating positive and negative peaks and the change of sign of the LID current with the sign change of the bias normal to the quantum-well plane. The quantitative estimates for GaAs wells show the LID current to be readily detectable.

### I. INTRODUCTION

The effect of light-induced drift (LID) in gas mixtures suggested in Ref. 1 manifests itself as a drift of absorbing particles in response to optical excitation with frequency close, but not exactly equal, to the resonant frequency of an internal transition in the particles. Characteristically, the spectral contour of LID is antisymmetric with respect to detuning from the internal transition frequency. LID has been observed<sup>2</sup> and studied in detail later (see, e.g., Ref. 3 and references cited therein).

The effect of LID is based on two features: (i) velocity-selective excitation of particles and (ii) dependence of the translational relaxation rate of the particles on their internal state. The velocity-selective excitation of particles is produced due to the Doppler shift. Consider, for instance, optical excitation redshifted with respect to the exact resonance. Then the particles that move toward the light source sense a blue Doppler shift which compensates the radiation detuning. Such particles are more likely to undergo excitation. As a result, their collision rate with a buffer gas, and consequently, the friction force acting upon them are changed. For the particles moving in the opposite direction, there is no excitation and no change of friction. Compelled by the imbalance in the friction forces for these two groups of particles, the absorbing component moves as a whole. The effect of surface LID predicted in Ref. 4 and observed in Ref. 5 is similar to the original LID but is based on collisions of the absorbing particles with the walls of the confining cell rather than with the buffer gas.

LID of electrons in semiconductors predicted in Refs. 6 and 7 and later observed<sup>8</sup> relies on parallel electron-energy bands in a quantizing magnetic field, where an electron moves freely in the field direction, and light excites transitions between the Landau levels. The translational motion of electrons in the field direction yields velocity-selective excitation, which can be interpreted in terms of the Doppler shift, as has originally been suggested in Ref. 9 (see also Ref. 10). Because the electron

translational relaxation depends on which of the Landau states the electron occupies, LID takes place.

Another case of parallel energy bands mentioned in Ref. 6 is that of electrons in two-dimensional quantum structures, such as inversion layers, thin films, etc., where the quantum state in the perpendicular direction plays the role of an internal state of the particle. Provided the translation relaxation depends on this state, LID occurs along the projection of the light wave vector  $\mathbf{k}$  onto the plane of the structure. However, no theory of such an effect is given in Ref. 6.

The photon drag effect (PDE) in semiconductor quantum wells has been suggested<sup>11,12</sup> and observed experimentally.<sup>13</sup> Like in Ref. 6, velocity-selective excitation in Refs. 11 and 12 is due to parallel subbands, and a difference of the lifetimes of the subband states is invoked, which makes this type of PDE similar to LID. Characteristically, this difference is due to optical phonon emission, which is energetically possible in the excited subband.<sup>11,13</sup>

The effect of LID in single quantum wells<sup>14</sup> is based on a different structure of the electron wave function in the normal direction, along the lines of Ref. 6. Specifically, the state-dependent relaxation in Ref. 14 is due to an increased intrusion of the electron wave function into the barrier regions in the excited subband (see also Ref. 15). Provided that the doping of the barrier and well regions is different, the scattering rate is different in the ground and excited subbands.

The present paper is devoted to the theory of the LID effect in coupled quantum wells. Such systems allow one to fully capitalize on the different structures of the wave functions in the ground and excited states to achieve state-dependent relaxation, which originates from quantum delocalization of the electron driven by resonant coherent tunneling between the wells. Because of the importance of polarization relaxation (dephasing), the density-matrix approach is invoked, similar to Ref. 14. The qualitative description of the effect and equations of motion for the density matrix are presented in Sec. II.

Analytical solutions and numerical examples are considered in Sec. III. The results are discussed in Sec. IV.

## II. QUALITATIVE DESCRIPTION AND DENSITY-MATRIX EQUATIONS

We consider the LID effect driven by electron delocalization over coupled quantum wells. This effect can exist in different quantum structures, where coherent tunneling of electrons between individual quantum wells is possible. For the sake of definiteness and simplicity, we restrict ourselves to the simplest of such structures, a double quantum well (Fig. 1). The excited state  $|2\rangle$  in the right well (numbered I in Fig. 1) and, say, the ground state  $|3\rangle$  in the left (II) well are aligned by the bias field as shown, or by the corresponding design of the double well to allow the resonant tunneling of electrons. The barrier regions are supposed to be modulation doped to yield the electron population of the structure and allow pure electronic intersubband transitions, which only will be considered.

One of the wells, say II, is supposed to be doped to create neutral scattering centers. When an electron is excited, by virtue of the resonant tunneling, it is delocalized over both the wells. The electron experiences more frequent collisions in the doped II well, resulting in faster translational relaxation in its excited state than in the overall ground state  $|1\rangle$ , because state  $|1\rangle$  is mainly localized in the undoped I well.

For the system under consideration, LID can be described as follows. The light has frequency close, but not exactly resonant, to the intersubband transition from the  $|1\rangle$  state to an excited state. Electrons move in the well plane due to their thermal motion for the nondegenerate electron gas or inside their Fermi surface for the degenerate gas. Those electrons for which the Doppler shift compensates the light detuning are excited, delocalize over the two wells, and, consequently, experience faster translational relaxation, i.e., greater friction force than

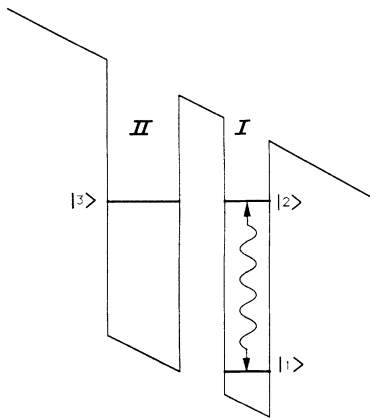


FIG. 1. Schematic of the coupled potential wells I and II. The overall ground state  $|1\rangle$  belongs in the I well. The excited state  $|2\rangle$  in the I well and the ground state  $|3\rangle$  in the II well are aligned by the bias. The optically excited intersubband transition is denoted by the wavy arrow.

the electrons moving in the opposite direction. Compelled by this force, the electron gas moves as a whole.

We emphasize that the effect is fundamentally based on quantum-mechanical delocalization, i.e., on the presence of an electron simultaneously in two wells. In this case, the collisions of electrons in the doped (II) well imply translational relaxation of the electron gas *as a whole*, which is required for LID. The quantum-mechanical delocalization over two wells is brought about by coherent tunneling, the condition for which is that the tunneling amplitude  $\tau$  is much greater than the polarization-relaxation rate  $\Gamma$ . In the opposite case  $|\tau| \ll \Gamma$ , the tunneling is incoherent, and the electron gas separates into two distinguishable weakly coupled components, one in the I well and the other in the II well. For both the components, the relaxation is not state dependent, and consequently LID is absent; albeit the concentration of electrons in the II well may be not very small as is the case in Ref. 16. In this respect, the present effects resemble the resistance resonance<sup>17</sup> and, similarly, can also be considered as an independent test of quantum mechanics.

The present effect differs from the phenomena described in Refs. 11 and 14 because it requires coherent tunneling and quantum delocalization of electrons between the wells. This brings about a different excitation spectrum and enhanced sensitivity to dephasing (polarization relaxation).

To describe the effect, we have to take into account the processes of intersubband excitation, the population, and polarization relaxation along with tunneling between the wells and the translational movement and relaxation in the plane of the quantum structure. As an adequate technique, we will use the quantum Liouville equation for the one-electron density matrix  $\rho_{ab}$  in the Wigner representation. This quantity is defined as

$$\rho_{ab}(\mathbf{p}, \mathbf{r}) = \sum_{\mathbf{q}} \exp(i\mathbf{q}\mathbf{r}) \rho_{ab}(\mathbf{p}, \mathbf{q}),$$

where  $\rho_{ab}(\mathbf{p}, \mathbf{q}) = \langle \alpha_{b, \mathbf{p} - (1/2)\mathbf{q}}^\dagger \alpha_{a, \mathbf{p} + (1/2)\mathbf{q}} \rangle$  is the Fourier transform<sup>18</sup> of  $\rho_{ab}(\mathbf{p}, \mathbf{r})$  over  $\mathbf{r}$ ,  $\alpha$  is the electron annihilation operator,  $a$  and  $b$  denote the states in the well ( $a, b = 1, 2, 3$ ),  $\mathbf{r}$  is the coordinate vector, and  $\mathbf{p}, \mathbf{q}$  are the momentum vectors that all lie in the plane of the wells.

The Hamiltonian of the electron plus an external optical field has the form

$$H = \sum_{a, \mathbf{p}} (\epsilon_a + \epsilon_{\mathbf{p}}) \alpha_{a, \mathbf{p}}^\dagger \alpha_{a, \mathbf{p}} + \sum_{a, b, \mathbf{p}, \mathbf{q}} U_{ab}(\mathbf{q}) \alpha_{a, \mathbf{p} + (1/2)\mathbf{q}}^\dagger \alpha_{b, \mathbf{p} - (1/2)\mathbf{q}},$$

where  $\epsilon_a$  is the energy of the  $a$ th level in the wells,  $\epsilon_{\mathbf{p}}$  is the electron kinetic energy, and  $U_{ab}(\mathbf{q})$  is the Fourier transform of the perturbation matrix element between states  $|a\rangle$  and  $|b\rangle$ . The independent nonzero matrix elements of the perturbation are

$$U_{21}(\mathbf{r}) = -\mathbf{d}_{21} [\mathbf{E} \exp(i\mathbf{k}\mathbf{r} - i\Omega t) + \text{c.c.}],$$

where  $\mathbf{d}$  is the dipole operator,  $\Omega$  is the frequency,  $\mathbf{k}$  is the wave vector, and  $\mathbf{E}$  is the electric-field amplitude of the light wave, and  $U_{32} = \tau$ , where the tunneling amplitude  $\tau$  coincides with the transfer integral  $t$  of Ref. 19.

The independence of  $\epsilon_p$  from the quantum state  $|a\rangle$  implies that the subbands in quantum wells are parallel, which is of principal importance for the theory, as discussed in Ref. 6.

The exact equation of motion for  $\rho$ , i.e., the quantum Liouville equation, can be obtained in a conventional way

$$i\frac{\partial\rho(\mathbf{p},\mathbf{r})}{\partial t}=[\epsilon,\rho(\mathbf{p},\mathbf{r})]+\sum_{\mathbf{q}}\exp(i\mathbf{q}\mathbf{r})(\epsilon_{\mathbf{p}+(1/2)\mathbf{q}}-\epsilon_{\mathbf{p}-(1/2)\mathbf{q}})\rho(\mathbf{p},\mathbf{q})+\sum_{\mathbf{q}}\exp(i\mathbf{q}\mathbf{r})[U(\mathbf{q})\rho(\mathbf{p}-\frac{1}{2}\mathbf{q},\mathbf{r})-\rho(\mathbf{p}+\frac{1}{2}\mathbf{q},\mathbf{r})U(\mathbf{q})]+iS. \quad (1)$$

In the first sum on the right-hand side of Eq. (1), the shift of  $\mathbf{p}$  by  $\pm\frac{1}{2}\mathbf{q}$  takes into account the velocity-selective excitation needed for LID, and such a shift describes the recoil effect in the second sum. As determined by  $U(\mathbf{q})$  in Eq. (1), the magnitude of  $\mathbf{q}$  is on the order of the photon momentum  $k$  and is much less than the typical electron momentum  $p$ . This justifies the lowest-order expansion in  $\mathbf{q}$  in Eq. (1). The first order in  $\mathbf{q}$  suffices for the first sum, and neglect of the recoil effect is possible in the second sum in Eq. (1), giving the quasiclassical Liouville equation

$$i\left[\frac{\partial}{\partial t}+\mathbf{v}\cdot\frac{\partial}{\partial\mathbf{r}}\right]\rho(\mathbf{p},\mathbf{r})=[\epsilon+U(\mathbf{r}),\rho]+iS, \quad (2)$$

where  $\mathbf{v}\equiv\partial\epsilon_p/\partial\mathbf{p}$  is the electron group velocity.

We employ the strong collision model for the population and translation relaxations and the relaxation-constant model for the dephasing, i.e., we adopt the following form of matrix  $S$ :

$$S_{11}=\gamma_I(n_1^{(0)}-n_1), \quad S_{22}=\gamma_I(n_2^{(0)}-n_2), \quad (3)$$

$$S_{33}=\gamma_{II}(n_3^{(0)}-n_3), \quad S_{ab}=-\Gamma_{ab}\rho_{ab} \quad \text{for } a\neq b.$$

Here  $n_a\equiv\rho_{aa}$  is the population of the  $|a\rangle$  state ( $a=1,2,3$ ),  $n_a^{(0)}$  is the equilibrium population of the  $|a\rangle$  state,  $n_a^{(0)}=[1+\exp(\epsilon_a+\epsilon_p-\epsilon_F)/T]^{-1}$ , where  $\epsilon_F$  is the Fermi energy,  $T$  is temperature,<sup>18</sup>  $\gamma_I$  and  $\gamma_{II}$  are the population relaxation constants (collision rates) in wells I and II, and  $\Gamma_{ab}$  is the polarization-relaxation constant for the transition  $|a\rangle\leftrightarrow|b\rangle$ , which is expressed in terms of the pure dephasing rate  $\bar{\Gamma}_{ab}$  in the form  $\Gamma_{ab}=\frac{1}{2}(\gamma_I+\gamma_{II})+\bar{\Gamma}_{ab}$ . Note that the condition  $\gamma_I\neq\gamma_{II}$  is necessary for the existence of the effect.

The structure of the diagonal matrix elements of  $S$  implies that an electron after a single collision (an event of interaction with the thermal bath) acquires the equilibrium populations  $n_a^{(0)}$ . It is worth noting that collision integral  $S$  in Eq. (3) does not conserve the total electron concentration, which is clear because  $\text{Tr}(S)\neq 0$  for  $\gamma_I\neq\gamma_{II}$ . This is a well-known general problem for the strong collision model. It is possible to overcome this problem and conserve the total electron concentration by introducing effective equilibrium concentrations  $n_a^{(0)*}$  as in Ref. 4. However, such a modification does not bring

by commuting the pair operator  $\alpha_{a,\mathbf{p}+(1/2)\mathbf{q}}^\dagger\alpha_{b,\mathbf{p}-(1/2)\mathbf{q}}$  with  $H$  and adding the relaxation matrix ("collision integral")  $S$  which arises from the interaction of an electron with the thermal bath represented by other electrons, scattering centers, and phonons. This equation has the form

about any substantial changes of the solutions. There is another possible interpretation, namely, that the total electron concentration may, indeed, be changed due to optical excitation. This is a likely situation in quantum wells because they are open systems in which the electrons are produced by outside donors and their equilibrium may be shifted by optical excitation. We accept this interpretation and will not modify  $S$ .

To solve Eq. (2), we will use the rotating-wave approximation (RWA), which is equivalent to retaining only terms in  $\rho$  with frequencies close to the exciting light frequency  $\Omega$  and neglecting multiple harmonics. This resonant approximation is well known to be good for a not too strong exciting wave, so that the field broadening of levels is much less than  $\Omega$ . In any case, if the exciting field is strong enough to violate the validity of the RWA, then the three-level scheme of Fig. 1 is not applicable, and excitation to higher levels and the continuum should be taken into account.

In the RWA, the space-time dependence of  $\rho_{ab}$  can be isolated in the form  $\rho_{12}=\bar{\rho}_{12}\exp(i\mathbf{k}\mathbf{r}-\Omega t)$ ,  $\rho_{13}=\bar{\rho}_{13}\exp(i\mathbf{k}\mathbf{r}-\Omega t)$ ,  $\rho_{23}=\bar{\rho}_{23}$ , where the amplitudes  $\bar{\rho}_{12}$ ,  $\bar{\rho}_{23}$ , and  $\bar{\rho}_{13}$  are slowly [with respect to  $\exp(i\mathbf{k}\mathbf{r}-\Omega t)$ ] varying functions of  $\mathbf{r}$  and  $t$ . The equations for these amplitudes follow from Eqs. (2) and (3):

$$\begin{aligned} \left[\frac{\partial}{\partial t}+\mathbf{v}\cdot\frac{\partial}{\partial\mathbf{r}}\right]n_1 &= 2\text{Im}(G\bar{\rho}_{12})+\gamma_I(n_1^{(0)}-n_1), \\ \left[\frac{\partial}{\partial t}+\mathbf{v}\cdot\frac{\partial}{\partial\mathbf{r}}\right]n_2 &= -2\text{Im}(G\bar{\rho}_{12}+\tau\bar{\rho}_{23}) \\ &\quad +\gamma_I(n_2^{(0)}-n_2), \\ \left[\frac{\partial}{\partial t}+\mathbf{v}\cdot\frac{\partial}{\partial\mathbf{r}}\right]n_3 &= 2\text{Im}(\tau\bar{\rho}_{23})+\gamma_{II}(n_3^{(0)}-n_3), \\ \left[\frac{\partial}{\partial t}+\mathbf{v}\cdot\frac{\partial}{\partial\mathbf{r}}\right]\bar{\rho}_{12} &= iG^*(n_2-n_1) \\ &\quad +i\tau\bar{\rho}_{13}-g_{12}\rho_{12}, \\ \left[\frac{\partial}{\partial t}+\mathbf{v}\cdot\frac{\partial}{\partial\mathbf{r}}\right]\rho_{13} &= iG^*\bar{\rho}_{23}+i\tau^*\bar{\rho}_{12}-g_{13}\bar{\rho}_{13}, \\ \left[\frac{\partial}{\partial t}+\mathbf{v}\cdot\frac{\partial}{\partial\mathbf{r}}\right]\bar{\rho}_{23} &= -i\tau^*(n_3-n_2) \\ &\quad +iG\bar{\rho}_{13}-g_{23}\bar{\rho}_{23}. \end{aligned} \quad (4)$$

Here  $g_{1a} = i(\Omega - \mathbf{k}\mathbf{v} - \varepsilon_{a1}) + \Gamma_{1a}$  and  $g_{ab} = -i\varepsilon_{ba} + \Gamma_{ab}$ , where  $a, b = 2, 3$ ,  $\varepsilon_{ab} = \varepsilon_a - \varepsilon_b$  is the transition frequency, and  $G = (d_z)_{12}E_z$  with the  $z$  axis perpendicular to the structure plane (note that  $|G|$  is the Rabi frequency). We point out that the Doppler shift  $\mathbf{k}\mathbf{v}$  in these formulas is not introduced phenomenologically, but rather appears as a result of a consistent theory derived in the RWA from the microscopic Hamiltonian.

The strong collision model for the collision integral  $S$  has been successfully used previously to describe LID in gas mixtures,<sup>1</sup> surface LID,<sup>4</sup> and LID in a single quantum well.<sup>14</sup> However, there is a problem in its application to double quantum wells and generally to systems with coherent quantum tunneling, which we would like to point out and discuss before using this model. This problem exists even without the light-wave field, i.e., for  $G = 0$ , in which case Eq. (4) can easily be solved for the two upper levels ( $a = 2, 3$ ) giving

$$n_a = \frac{n_a^{(0)} + 2|\tau|^2 \Gamma_{23}(\varepsilon_{23}^2 + \Gamma_{23}^2)^{-1}(n_2^{(0)}\gamma_{II}^{-1} + n_3^{(0)}\gamma_I^{-1})}{1 + 2|\tau|^2 \Gamma_{23}(\varepsilon_{23}^2 + \Gamma_{23}^2)^{-1}(\gamma_{II}^{-1} + \gamma_I^{-1})} \quad (5)$$

$$|\rho_{23}|^2 = (n_2 - n_3)^2 |\tau|^2 (\varepsilon_{23}^2 + \Gamma_{23}^2)^{-1}.$$

The problem mentioned above is evident in the case of completely coherent tunneling, i.e., for  $|\tau| \gg \Gamma_{23}$ . In this case, states  $|2\rangle$  and  $|3\rangle$  are mixed to form new stationary states  $|+\rangle$  and  $|-\rangle$  with energies

$$\varepsilon_{\pm} = \frac{1}{2}[\varepsilon_2 + \varepsilon_3 \pm (\varepsilon_{23}^2 + 4|\tau|^2)^{1/2}].$$

The populations of these states  $n_+$  and  $n_-$  can be found as the eigenvalues of  $\rho$ , Eq. (5), in the form

$$n_{\pm} = \frac{1}{2} \left[ n_2 + n_3 \pm (n_2 - n_3) \left( 1 + \frac{4|\tau|^2}{\varepsilon_{23}^2 + \Gamma_{23}^2} \right)^{1/2} \right]. \quad (6)$$

The problem is that in the generic case the populations  $n_{\pm}^{(0)}$ , Eq. (6), do not conform to equilibrium because they do not have the required form of the Fermi distribution  $n_{\pm} = [1 + \exp(\varepsilon_{\pm} + \varepsilon_p - \varepsilon_F)/T]^{-1}$ , provided that the populations  $n_a^{(0)}$  do [see text following Eq. (3)].

However, as we show below, this problem is eliminated in limiting cases that are determined by the validity of at least one of the following three inequalities:

$$|\varepsilon_{23}| \gg |\tau|, \quad (7)$$

$$\varepsilon_{21}, \varepsilon_{31} \gg T, |\tau|, \quad (8)$$

$$T \gg |\tau|. \quad (9)$$

Let us consider these three cases in some detail. (i) The inequality in Eq. (7) means a large mismatch of levels and ensures that the mixing of states  $|2\rangle$  and  $|3\rangle$  is small. In this case, from Eq. (6) we obtain  $n_+ \approx n_2^{(0)}$  and  $n_- \approx n_3^{(0)}$ , i.e., the populations  $n_{\pm}$  are the equilibrium ones. (ii) From Eq. (8) it follows that both the  $|\pm\rangle$  levels are almost unpopulated, confirming to equilibrium. (iii) In the case of Eq. (9), two subcases are possible. First, if  $|\varepsilon_{23}| \ll T$ , then from Eqs. (5) and (6) it follows that  $n_+ \approx n_- \approx n_2^{(0)} \approx n_3^{(0)}$ , as expected for the equilibrium. Second, if  $|\varepsilon_{23}| \gtrsim T$ , then we return to the case of Eq. (7).

The inequalities (7)–(9) do not contradict each other. We point out that any or all of these conditions may be valid experimentally. For instance, setting realistic values (see Ref. 16 for the details of computing these values) for GaAs quantum wells of  $\sim 100$  Å thickness as  $\tau \approx 0.5$  meV,  $\varepsilon_{21} \approx \varepsilon_{31} \approx 30$  meV, and  $T \approx 5$  meV (60 K), we conclude that both Eqs. (8) and (9) are valid. This justifies the use of the collision integral (3).

### III. SOLUTIONS AND NUMERICAL ILLUSTRATIONS

From symmetry considerations, the LID current is directed along the projection of  $\mathbf{k}$  onto the quantum structure plane (say, along the  $x$  direction). Its density  $j$  can be expressed in terms of the solution of Eq. (4) in two equivalent forms:

$$j = e \int v_x (n_1 + n_2 + n_3) d\mathbf{p} / (2\pi)^2$$

$$= e (1 - \gamma_{II}/\gamma_I) \int v_x n_3 d\mathbf{p} / (2\pi)^2, \quad (10)$$

where  $v_x = \partial \varepsilon_p / \partial p_x$  is the  $x$  component of electron velocity and  $e$  is the electron charge. The second expression in Eq. (10) corroborates the fact that the driving force of LID in the system considered originates from the difference of the relaxation rates in wells I and II.

The part of the homogeneous stationary solution of Eq. (4) needed to find the current (10) can be exactly found as

$$n_3 = \frac{n_3^{(0)}D + n_2^{(0)}\gamma_I(B - A) + n_1^{(0)}\gamma_I A + (n_1^{(0)} + n_2^{(0)} + n_3^{(0)})\gamma_{II}/\gamma_I(BC - A^2)}{D + \gamma_I B + (2 + \gamma_{II}/\gamma_I)(BC - A^2)}, \quad (11)$$

where  $D = \gamma_I \gamma_{II} + \gamma_{II}[B + 2(C - A)]$  and

$$A \equiv 2|\tau G|^2 \text{Re}(F^{-1}),$$

$$B \equiv 2|\tau|^2 \text{Re}[(g_{12}g_{13} + |\tau|^2)F^{-1}],$$

$$C \equiv 2|G|^2 \text{Re}[(g_{13}g_{23} + |G|^2)F^{-1}],$$

$$F \equiv g_{23}(g_{12}g_{13} + |\tau|^2) + g_{12}|G|^2.$$

Let us consider some limiting cases of the solution (11). In the absence of tunneling ( $\tau \rightarrow 0$ ),  $n_3 = n_3^{(0)}$  and, consequently, LID is absent as expected, because the effect is

driven by quantum delocalization due to tunneling. In the optically nonsaturated case, which is determined by the condition  $|G|^2 \gamma_I^{-1} \Gamma_{12}^{-1} \ll 1$ , we see from Eqs. (10) and (11) that  $j \propto |G|^2$ , i.e., the LID current is proportional to

$$n_3 - n_3^{(0)} = 2|G\tau|^2 (n_1^{(0)} - n_2^{(0)}) \frac{2c\Gamma_{23} + a\gamma_I(\varepsilon_{32}^2 + \Gamma_{32}^2)}{\gamma_I\gamma_{II}(\varepsilon_{32}^2 + \Gamma_{32}^2) + 2|\tau|^2\Gamma_{23}(\gamma_I + \gamma_{II})}, \quad (12)$$

$$a \equiv \text{Re}(f^{-1}), \quad c \equiv \text{Re}(g_{13}g_{23}f^{-1}), \quad f \equiv g_{23}(g_{12}g_{13} + |\tau|^2).$$

For the large level mismatch  $|\varepsilon_{32}| \gg \Gamma_{32}$ , the LID current [see Eqs. (11) and (12)] tends to zero, as expected for an effect driven by resonance tunneling. It can be easily seen from Eq. (12) that when the temperature is relatively high  $T \gg \varepsilon_{21}$ , the LID current vanishes by virtue of  $n_1^{(0)} - n_2^{(0)} \rightarrow 0$ . Since for the nondegenerate gas LID also vanishes for  $T \rightarrow 0$  because of  $v \rightarrow 0$ , it is clear that there exists an optimum temperature  $T_o \sim \varepsilon_{21}$ .

It is possible to obtain an analytical expression for the LID current only in a special case, which we consider below. We adopt optically nonsaturated conditions. Also, we assume the effective mass  $m^*$  to determine the electron dispersion by setting  $\mathbf{v} = \mathbf{p}/m^*$ , and suppose the electron gas to be nongenerate using the Maxwell-Boltzman distribution

$$n_a^{(0)}(\mathbf{v}) \propto N \exp(-\varepsilon_a/T - v^2/v_i^2),$$

where  $v_i = (2T/m^*)^{1/2}$  is the thermal velocity and  $N$  is the 2D density of electrons. Additionally, we assume that the tunneling is coherent, i.e.,  $|\tau| \gg \Gamma_{12}, \Gamma_{13}, \Gamma_{23}$ .

In this case the LID profile (12) consists of two non-overlapping contours  $j_{\pm}$  arising from the excitation of the corresponding components  $|\pm\rangle$  of the split doublet. Each of these contours centers about the corresponding transition frequency

$$\varepsilon_{\pm 1} = \frac{1}{2}[\varepsilon_{21} + \varepsilon_{31} \pm (\varepsilon_{23}^2 + 4|\tau|^2)^{1/2}].$$

From Eqs. (10) and (12) we obtain

$$j_{\pm} = 2\pi^{3/2} I e N K_{\pm} \Omega^{-1} |d_z|_{12}^2 (\gamma_{II}^{-1} - \gamma_I^{-1}) Z^{-1} \times [1 - \exp(-\varepsilon_{21}/T)] C(\xi_{\pm}) \cos^2 \theta, \quad (13)$$

where  $Z = \sum_a \exp(-\varepsilon_{a1}/T)$  is the partition function,  $I$  is light intensity,  $d_z$  is the normal component of the electron dipole operator,  $\theta$  is the angle between the light-polarization vector and the  $z$  direction (the normal to the well plane), and  $K_{\pm}$  are dimensionless coefficients and  $C$  is a function<sup>14</sup> of the complex arguments  $\xi_{\pm}$  defined as

$$K_{\pm} = \pm 4|\tau|^2 \gamma_I^{-1} (\varepsilon_{23}^2 + 4|\tau|^2)^{-1/2} [2\Gamma_{23}(\varepsilon_{\pm 1} - \varepsilon_{21}) + \varepsilon_{23}\gamma_I] \times [\varepsilon_{23}^2 + 2|\tau|^2\Gamma_{23}(\gamma_I^{-1} + \gamma_{II}^{-1})]^{-1},$$

$$C(\xi) = \text{Re}\{\xi \exp(-\xi^2) [1 + \text{erf}(i\xi)]\}, \quad (14)$$

$$\xi_{\pm} = (\Omega - \varepsilon_{\pm 1})/kv_t + i\Gamma_{\pm}/kv_t,$$

$$\Gamma_{\pm} \equiv \pm [\Gamma_{13}(\varepsilon_{\pm 1} - \varepsilon_{21}) + \Gamma_{12}(\varepsilon_{\pm 1} - \varepsilon_{31})] (\varepsilon_{32}^2 + 4|\tau|^2)^{-1/2}.$$

the light intensity, as expected. The analytical expression for this limiting case is cumbersome. To simplify it, we set  $n_2^{(0)} = n_3^{(0)}$  [see Eq. (9) and the discussion after it] and obtain from Eq. (11)

Each of the contours in Eq. (14),  $j_+$  and  $j_-$ , has the same antisymmetric form with respect to its central frequency  $\varepsilon_{\pm 1}$  as for LID in a single well.<sup>14</sup> However, the magnitudes of these contours are different, determined by the  $K_{\pm}$  coefficients. In the case of exact level matching,  $\varepsilon_{23} = 0$ , Eq. (14) is greatly simplified, giving

$$K_{\pm} = \gamma_{II}/(\gamma_I + \gamma_{II}), \quad \Gamma_{\pm} = \frac{1}{2}(\Gamma_{13} + \Gamma_{12}). \quad (15)$$

In this case,  $K_{\pm}$  and  $\Gamma_{\pm}$  do not depend on  $\tau$  and on the  $|\pm\rangle$  state index. Consequently, the LID current (13) does not depend on the interwell-barrier thickness, which is the principal property of the coherent tunneling regime.

Let us consider numerical illustrations for the structure shown in Fig. 1 in the effective-mass model for the nondegenerate electron gas adopting the following realistic parameters:  $m^* = 0.067m$  ( $m$  is the free-electron mass),  $\varepsilon_{21} = 30$  meV,  $\gamma_I = 0.1$  meV,  $\gamma_{II} = 0.2$  meV, and  $|\tau| = 1$  meV. These correspond<sup>16</sup> to the GaAs wells with a width of 150 Å for the I well, and the Al<sub>0.1</sub>Ga<sub>0.9</sub>As central barrier with a thickness 80 Å. The temperature  $T$  is set in the calculations as 10 meV (116 K).

Figure 2 displays the spectral profiles of the LID current for different polarization-relaxation rates in the optically nonsaturated regime with exact level alignment ( $\varepsilon_{23} = 0$ ). These profiles are calculated with Eqs. (10) and (12) in terms of the drift velocity  $v_d = j/eN$  normalized to  $v_i$  and to  $|G|^2$  (meV<sup>2</sup>) to exclude the light intensity.

For the case  $\Gamma_{ab} \ll |\tau|$  (weak polarization relaxation or nearly coherent tunneling), the LID profile [see Fig. 2(a)] consists of two nonoverlapping dispersion-type contours. Both these contours are antisymmetric with respect to the corresponding centers which are positioned at the transition frequencies of the split doublet levels  $\varepsilon_{\pm 1}$ . These contours are quantitatively described by the terms  $j_+$  and  $j_-$  of Eq. (13). As the calculations show, in the case under consideration the LID profile does not significantly depend on  $\tau$ , i.e., on the interwell-barrier thickness, as expected for coherent tunneling [see the discussion of Eq. (15)].

For intermediate polarization relaxation  $\Gamma_{ab} \sim |\tau|$ , Fig. 2(b) demonstrates that the contours are overlapped, and the antisymmetry with respect to their centers is lost. The magnitude of the LID current is decreased 20 times, while the increase of  $\Gamma_{ab}$  is only fivefold. This drastic decrease of  $v_d$  is indicative of the separation of the electron gas into two distinguishable gases localized in the wells I

and II, as discussed above. A further fivefold increase of  $\Gamma_{ab}$  [see Fig. 2(c)] causes complete disappearance of the two-contour structure, which is replaced by a single dispersion-type antisymmetric profile centered near the transition frequency  $\varepsilon_{21}$  in the I well, as expected for completely incoherent (stepwise) tunneling. The LID current is further reduced 20-fold, manifesting nearly complete loss of quantum coherence and separation of the electron gas into two almost uncoupled distinguishable components. These findings directly confirm the

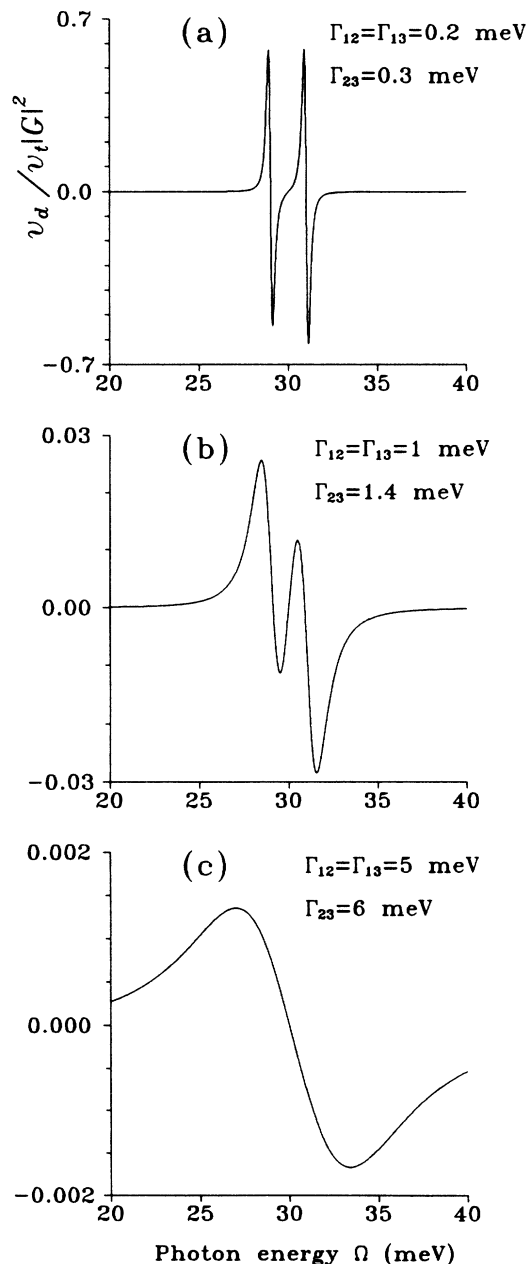


FIG. 2. Spectral profiles of the normalized LID velocity for the polarization-relaxation constants  $\Gamma_{12}$  and  $\Gamma_{13}$  as indicated in the figures, with  $\Gamma_{23} = 1.4\Gamma_{12}$ . Other parameters are given in the text.

coherent quantum nature of the effect. Note that the intermediate relaxation case illustrated in Fig. 2(b) is often realistic experimentally.

The dependence of the LID spectral profiles on the level mismatch  $\varepsilon_{23}$  calculated from Eqs. (10) and (12) is presented in Fig. 3, where the series of curves is shown with  $\varepsilon_{21} = \text{const}$  and  $\varepsilon_{31}$  being increased. The curve for the case of perfect matching ( $\varepsilon_{23} = 0$ ) is the same as in Fig. 2(b). The change in profile with an increase of the mismatch is rather nontrivial. For moderate mismatch,  $\varepsilon_{23} = 2$  meV, the left (“red”) component of the profile, which corresponds to the transition  $|1\rangle \rightarrow |-\rangle$ , is broadened and blue-shifted, and its amplitude is increased. The last feature is counterintuitive, because the effect is driven by the quantum tunneling which is suppressed with the level-mismatch increase. The enhancement of the LID in this case is the result of the increased localization of the  $|-\rangle$  state wave function in the I well. This localization brings about better overlap of the wave functions in the ground state  $|1\rangle$  and the excited state  $|-\rangle$ , which results in an increase in the strength of the dipole transition  $|1\rangle \rightarrow |-\rangle$ . Another reason for the LID enhancement is the increase of the electron lifetime in the  $|-\rangle$  state, because of the electron localization in the undoped well I with low collision rate. These two factors bring about the increase of the  $|-\rangle$  state population and, consequently, LID, counteracting the decrease in the tunneling caused by the intermediate mismatch.

The right (“blue”) component of the profile (Fig. 3), which corresponds to the transition  $|1\rangle \rightarrow |+\rangle$ , in all cases is strongly diminished with the mismatch. This is because the  $|+\rangle$  wave function localizes in the II well, and all the factors mentioned above bring about a decrease of LID. When the mismatch becomes large ( $\varepsilon_{32} = 8$  meV), both the left and right components of the LID spectral profile decrease in magnitude due to the diminished tunneling. However, the right component decreases much more, in accord with the discussion above. In the case of the large mismatch, the left and right components of the spectral profile are centered at the transi-

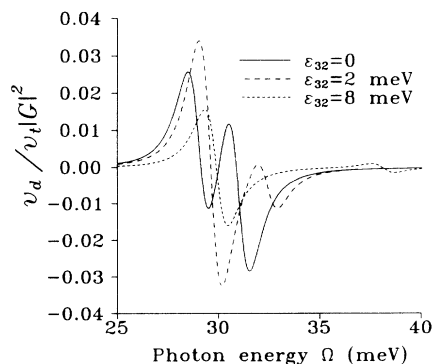


FIG. 3. LID spectral profiles plotted for different values of the level mismatch  $\varepsilon_{32}$ , as shown in the graph, with  $\varepsilon_{21} = 30$  meV. The relaxation constants are  $\Gamma_{12} = \Gamma_{13} = 1$  meV,  $\Gamma_{23} = 1.4$  meV.

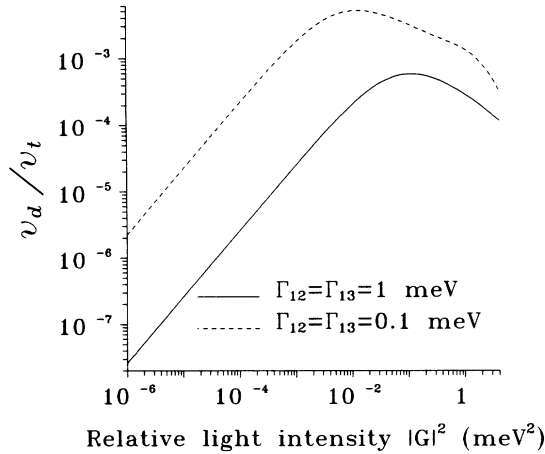


FIG. 4. LID velocities plotted against  $|G|^2$ . The quantity  $|G|^2$  is proportional to the light intensity, and  $|G|^2 = 1 \text{ meV}^2$  approximately corresponds to  $I = 30 \text{ kW/cm}^2$ . The constants  $\Gamma_{12}$  and  $\Gamma_{23}$  are indicated in the figure, and  $\Gamma_{13} = 1.4\Gamma_{12}$ . Note the double logarithmic scale.

tion frequencies in uncoupled wells,  $\epsilon_{21}$  and  $\epsilon_{31}$ , as expected.

The dependence of the drift velocity on  $|G|^2$ , i.e., on the light intensity, calculated with Eqs. (10) and (11) is shown in Fig. 4. This dependence at small intensities is linear in accord with Eqs. (12) and (13), then reaches its maximum and starts to decrease sharply due to field broadening of the levels. With the increase of dephasing (cf. the dashed and solid curves), the current reaches a lower maximum value at higher intensities, which is due to the separation of the electron gas into two distinguishable components, as discussed above, and diminished velocity selectivity of the excitation. For the realistic values  $\Gamma_{12} = \Gamma_{13} = 1 \text{ meV}$ , the maximum LID current occurs at  $|G|^2 \approx 0.1 \text{ meV}^2$ , corresponding to the light intensity  $I \approx 3 \text{ kW/cm}^2$ , which is easily reachable experimentally [as an estimate, we adopted  $(d_z)_{12} = 30 e \text{ \AA}$ ]. The maximum drift velocity is fairly high,  $v_d \approx 2 \times 10^{-4} v_t$ . For a typical 2D electron density  $N \sim 2 \times 10^{10} \text{ cm}^{-2}$  and well width (in the  $y$  direction)  $L = 0.1 \text{ cm}$ , this yields the total current per double well of  $J = eNLv_d \approx 1 \text{ \mu A}$ , which is indeed easily detectable.

#### IV. DISCUSSION

The theory of the effect of light-induced drift (LID) of electrons is presented in this paper. Both qualitative and quantitative properties of the effect are discussed above in Secs. II and III, in particular, in connection with the numerical illustrations (Figs. 2–4). Here we do not attempt to repeat this discussion, but rather pursue two alternative interrelated goals, namely, to show the place of this effect among other electron-transfer and photocurrent effects in quantum wells, and to indicate the features of the effect which may be useful for its experimental observation and identification.

LID in coupled wells requires the tunneling of electrons between wells. Among the large number of effects

involving such tunneling, most are based on any type of tunneling, coherent or incoherent (stepwise). The transfer of an electron is what is observed, usually by recording photoluminescence spectra (see, e.g., Refs. 20 and 21). In such experiments, the specific mechanism of tunneling manifests itself only through the tunneling rate and its dependence on the barrier thickness. In this connection, we point out that even incoherent tunneling in some realistic cases can yield an appreciable electron transfer.<sup>16</sup> However, the coherence of tunneling is an essential property for time-resolved experiments, including a recent one<sup>22</sup> in which coherent electron oscillations have been observed.

The present effect manifests itself as the lateral stationary photocurrent which depends on coherent tunneling between wells. The coupling of lateral and normal movement induced by the optical excitation makes LID unique. Once again, we emphasize that coherent tunneling is required, because collisions in one (doped) well should transfer momentum to the electron gas as a whole. In contrast to this, incoherent tunneling brings about separate existence of two distinguishable electron gases in the different wells, in which case the collision rate is not state dependent and LID is absent.

There is another effect, namely, the resistance resonance,<sup>17</sup> which is also based on the coupling of lateral and transverse motion and requires coherent tunneling. However, the effect of Ref. 17 is purely electric, there is no light, and intersubband transitions and excited electronic states do not participate. Consequently, different tunneling and relaxation processes contribute. There is another important distinction of LID. When there is no coherent tunneling, LID is absent. By contrast, the tunneling changes resistance typically by  $\sim 20\%$  only.<sup>17</sup> Therefore, distinct from the resistance resonance, LID in the coupled quantum wells is a background-free probe for coherent tunneling. Note that different rates of polarization relaxation, i.e., different degrees of tunneling coherence, correspond to essentially different forms of the LID profiles (see Fig. 2). Therefore, LID allows one to obtain quantitative information on the tunneling coherence.

Now we discuss the features of LID in the coupled wells pertinent to its experimental observation. As estimated at the end of Sec. III, the maximum current is achieved under rather low light intensity ( $\sim 1 \text{ kW/cm}^2$ ) and is comparatively large,  $J \approx 1 \text{ \mu A}$ . We emphasize that this is the current induced in one double well. Certainly, such a current is easily detectable. The fundamental property<sup>14</sup> of the LID current in a single quantum well of being antisymmetric with respect to the detuning from the intersubband-transition center is absent for two coupled wells in the generic case. However, as inspection of Eqs. (10) and (11) shows, in the case of exact level matching ( $\epsilon_{23} = 0$ ), the spectral profile of LID is almost antisymmetric with respect to the frequency  $\epsilon_{21} = \epsilon_{31}$ , i.e., to the center of the split doublet. This property can be easily traced in Fig. 2.

Another distinctive feature of the effect is that it changes its sign if well I, and not II, is doped. Of course, it is not necessary to have a different specimen with another well doped. It is sufficient to change the bias sign

to have the optical excitation in the doped well. This is equivalent to switching wells I and II (see Fig. 1), which changes the sign of the current. It is advantageous experimentally to have a geometrically symmetric double well with one of the individual wells doped. The double well should be biased so that the ground state in one well is aligned with the first excited state in the other well achieving the scheme shown in Fig. 1. When the bias reverses its sign, the current also does.

We point out the importance of the alignment of the excited level in one well with the ground state in the other, as shown in Fig. 1. Such a scheme excludes the counterfield electron transfer<sup>16</sup> which may have inter-

ferred with LID if two excited states were aligned.

The response-relaxation time of LID, as follows from inspection of Eq. (4), is on the order of the reciprocal collision rates  $\gamma_I^{-1}, \gamma_{II}^{-1}$ . Consequently, the realistic values of this time are on a subpicosecond scale. Such a fast response makes LID in double quantum wells promising for applications.

#### ACKNOWLEDGMENT

This research has been supported by the Office of Naval Research.

\*Also at Institute of Automation and Electrometry, Russian Academy of Sciences, Novosibirsk 630090, Russia.

<sup>1</sup>F. Kh. Gel'mukhanov and A. M. Shalagin, *Pis'ma Zh. Eksp. Teor. Fiz.* **29**, 773 (1979) [*JETP Lett.* **29**, 711 (1979)].

<sup>2</sup>V. D. Antsygin, S. N. Atutov, F. Kh. Gel'mukhanov, G. G. Telegin, and A. M. Shalagin, *Pis'ma Zh. Eksp. Teor. Fiz.* **30**, 262 (1979) [*JETP Lett.* **30**, 243 (1979)].

<sup>3</sup>H. G. C. Werij, J. E. M. Haverkort, P. C. M. Planken, E. R. Eliel, J. P. Woerdman, S. N. Atutov, P. L. Chapovski, and F. Kh. Gel'mukhanov, *Phys. Rev. Lett.* **58**, 2660 (1987).

<sup>4</sup>A. V. Ghiner, M. I. Stockman, and V. A. Vaksman, *Phys. Lett.* **96A**, 79 (1983).

<sup>5</sup>R. W. M. Hoogeveen, R. J. C. Spreeuw, and L. J. F. Hermans, *Phys. Rev. Lett.* **59**, 447 (1987).

<sup>6</sup>A. M. Dykhne, V. A. Roslyakov, and A. N. Starostin, *Dok. Akad. Nauk SSSR* **254**, 599 (1980) [*Sov. Phys. Dokl.* **25**, 741 (1980)].

<sup>7</sup>E. M. Skok and A. M. Shalagin, *Pis'ma Zh. Eksp. Teor. Fiz.* **32**, 201 (1980) [*JETP Lett.* **30**, 184 (1980)].

<sup>8</sup>A. V. Kravchenko, A. M. Pakin, V. N. Sozinov, and O. A. Shegai, *Pis'ma Zh. Eksp. Teor. Fiz.* **38**, 328 (1983) [*JETP Lett.* **38**, 393 (1983)].

<sup>9</sup>L. E. Gurevich and A. Ya. Vinnikov, *Fiz. Tverd. Tela* **15**, 87 (1973) [*Sov. Phys. Solid State* **15**, 58 (1973)].

<sup>10</sup>The optoelectric effect considered in Ref. 9 does not invoke a difference in the relaxation rates of the Landau levels and, consequently, is not LID. In particular, its spectral contour does not possess an antisymmetric form characteristic of LID (see also the discussion in Ref. 15).

<sup>11</sup>S. Luryi, *Phys. Rev. Lett.* **58**, 2263 (1987).

<sup>12</sup>A. A. Grinberg and S. Luryi, *Phys. Rev. B* **38**, 87 (1988).

<sup>13</sup>A. D. Wieck, H. Sigg, and K. Ploog, *Phys. Rev. Lett.* **64**, 463 (1990).

<sup>14</sup>M. I. Stockman, L. N. Pandey, and T. F. George, *Phys. Rev. Lett.* **65**, 3433 (1990).

<sup>15</sup>M. I. Stockman, L. N. Pandey, and T. F. George, *Phys. Rev. Lett.* **67**, 157 (1991).

<sup>16</sup>M. I. Stockman, L. S. Muratov, L. N. Pandey, and T. F. George, *Phys. Lett.* **163A**, 233 (1992); *Phys. Rev. B* **45**, 8550 (1992).

<sup>17</sup>A. Palevski, F. Capasso, L. Pfeiffer, and K. W. West, *Phys. Rev. Lett.* **65**, 1929 (1990).

<sup>18</sup>For simplicity of notation, we use the system of units in which  $\hbar=1$  and no distinctions are made between wave vectors and momenta and also between energies and frequencies. The Fourier transforms are denoted by indicating a momentum variable in place of the corresponding coordinate variable. We express temperature in energy units, i.e., set the Boltzmann constant  $k_B=1$ .

<sup>19</sup>G. Bastard, *Wave Mechanics Applied to Semiconductor Heterostructures* (Les Editions de Physique, Les Ulis, France, 1988).

<sup>20</sup>R. Sauer, K. Thonke, and W. T. Tsang, *Phys. Rev. Lett.* **61**, 609 (1988).

<sup>21</sup>B. Deveaud, F. Clerot, A. Chomette, A. Regreny, R. Ferreira, G. Bastard, and B. Sermage, *Europhys. Lett.* **11**, 367 (1990).

<sup>22</sup>K. Leo, J. Shah, E. Göbel, T. Damen, S. Schmitt-Rink, and W. Schäfer, *Phys. Rev. Lett.* **66**, 201 (1991).